https://doi.org/10.5194/egusphere-2026-1437
Preprint. Discussion started: 30 March 2026

Role of diatoms reproductive dynamics in plankton trophic webs

Paolo Lazzari[1,2], Francesco Dattilo[3], Ivano Vascotto[1], Alberto Ghedin[1,2], Guido Occhipinti[4], and Eva Álvarez[5]

[1]National Institute of Oceanography and Applied Geophysics - OGS, Italy
[2]NBFC, National Biodiversity Future Center, Italy
[3]CMCC Foundation - Euro-Mediterranean Center on Climate Change, Italy
[4]MARBEC, Univ Montpellier, CNRS, Ifremer, IRD, Sète, France
[5]Instituto Español de Oceanografía (IEO-CSIC), Centro Oceanográfico de Gijón/Xixón, Spain

Correspondence: Paolo Lazzari (plazzari@ogs.it)

Abstract. Diatoms are key contributors to marine biogeochemical cycles, yet their distinctive reproductive strategies are rarely represented explicitly in ecosystem and biogeochemical models. In particular, the alternation between asexual size reduction and sexual size restitution introduces intrinsic size-structured dynamics that may influence plankton community structure and biodiversity. Here we incorporate a size-structured formulation of diatom reproductive dynamics into a coupled optical–biogeochemical plankton model to assess their impact on plankton biomass, diversity, and trophic interactions.

The model represents size-dependent asexual reproduction as a shrinking flux across diatom size classes and sexual reproduction as a restitution process activated below a critical size threshold. Using long-term simulations and a Monte Carlo ensemble exploring uncertainty in reproductive parameters, we evaluate the sensitivity of plankton communities to variations in reproduction rates.

Results show that asexual reproduction exerts a dominant control on diatom biomass and size structure, producing nonlinear, threshold-like responses capable of reorganizing phytoplankton functional composition and propagate upward through the food web. Sexual reproduction acts mainly as a secondary modulator, while trophic interactions buffer variability at higher trophic levels. These findings highlight reproductive dynamics as important regulators of plankton biodiversity and biogeochemical functioning.

1 Introduction

Biodiversity is the sum of all living things on earth and their interactions. It is an enormously complicated mechanism whose results are breathable air, drinkable water and a clean a sustainable environment. Recent generations of marine biogeochemical models are increasingly moving beyond coarse functional-type representations to incorporate trait-based descriptions that explicitly resolve key optical and size-related properties of phytoplankton (Álvarez et al., 2025; Dutkiewicz et al., 2020). In these frameworks, phytoplankton groups such as diatoms, dinoflagellates, and cyanobacteria are no longer treated as homogeneous functional classes, but are characterized by size-dependent physiological rates, light-harvesting and photoadaptive traits, and variable trophic interactions. The explicit inclusion of optical traits links phytoplankton physiology to the underwater light field, while size structure governs nutrient uptake, growth, grazing susceptibility, and export efficiency. Together, these

https://doi.org/10.5194/egusphere-2026-1437
Preprint. Discussion started: 30 March 2026

trait-based formulations enable the emergence of more realistic and dynamically complex trophic networks, in which energy and matter flow across multiple size classes and functional groups, thereby strengthening the coupling between ecosystem structure and biogeochemical cycling (Ward et al., 2012; Dutkiewicz et al., 2020). Although size-structured trait-based models substantially improve the representation of plankton community structure, they generally assume fixed size classes. Growth is therefore represented implicitly through changes in biomass within size classes, rather than through explicit cell growth and division. As a result, ontogenetic trajectories and life-history processes of individual organisms, especially phytoplankton, are not explicitly accounted for. There are modelling efforts in the literature that explicitly include ontogenetic or life-stage structure of organisms, especially via multicellular zooplankton such as copepods (i.e.; Clerc et al., 2024), or "end-to-end" ecosystem models linking physical/biogeochemical models with explicit population models for fish and higher trophic levels, often including ontogenetic development and individual behaviour (i.e.; Johanson et al., 2017). However, the impact on aggregated biogeochemical functions (e.g., carbon export, nutrient cycling) are still under investigation. These type of efforts are still relatively rare in the phytoplankton component of biogeochemical ocean models, that most of the time treat organisms as functional pools without explicit life history.

Diatoms are unicellular planktonic organisms which occupy a wide range of body size and cell biovolume which spans along nine orders of magnitude (Litchman et al., 2009; Sieburth et al., 1978). But diatoms cell size also varies among the individual components of the same species, which it is connected to a key feature of this taxonomical group: a siliceous exoskeleton composed of two frustules fitting each other (Reynolds, 2006). The frustules composing the diatoms body are of fixed size and will be donated to the daughter cells as the asexual reproduction occurs. Since one of the frustules is smaller than the other, one of the two daughter diatoms will be smaller along the apical axes at each reproduction cycle. The net result of this process is the reduction in size of the whole diatom community as this becomes more abundant. To restore the population to the original size a common strategy is sexual reproduction. Centric diatoms are generally homotallic, that is a single clone can produce both eggs and sperm, while most pennate diatoms are heterothallic, which means sexual reproduction requires a pair of opposite mating types. The onset of the sexual phase is purely physical: microsurgery experiments showed that newborn cells shrunk below their sexualization size threshold (SST) acquire sexual competence (Stosch, 1965; Roshchin and Khauilov, 1994; Chepurnov et al., 2004). As the cells become smaller, they increase the chance of sexual reproduction. With sexual mating the reproductive cycle concludes, and two cell form one (centric diatoms) or two (pennate diatoms) auxospores (Drebes, 1977). The auxospore will grow forming inside itself a new specimen of the maximal size. This new diatom cell will then reproduce again asexually. The whole cycle is known as cell size reduction–restitution cycle (SRRC, Hense and Beckmann, 2015).

Cell size has a major influence on the ecology of diatoms, as this property affects the susceptibility to grazing, the sinking rate, and the optimal concentration of nutrient (Reynolds, 2006). Lastly, as mentioned above cell size has a key role in diatom physiological processes of sexualisation and it acts as an internal non-genetic factor (Drebes, 1977). In marine biogeochemical cycles, diatoms play an important role in structuring planktonic communities and driving ecosystem functioning. Although they account for roughly 25% of global ocean net primary production, diatoms often dominate phytoplankton assemblages in many regions and seasons. Their distinct physiological and ecological traits, including rapid growth rates and strong responses to nutrient inputs, make them key contributors to primary production and biogeochemical variability.

https://doi.org/10.5194/egusphere-2026-1437
Preprint. Discussion started: 30 March 2026

This study explicitly incorporates diatom reproductive dynamics into a moderately complex, trait-based biogeochemical ecosystem model. By embedding size-structured asexual and sexual reproduction processes within a coupled optical–biogeochemical framework, this work moves beyond idealized or population-level formulations and allows reproductive strategies to interact dynamically with trophic structure, biodiversity, and elemental cycling. Therefore, this approach provides a pathway for linking diatom life-cycle processes to emergent ecosystem-level behavior in marine biogeochemical models. This manuscript is organized as follows. Section 2 introduces the theoretical framework used to describe diatom reproductive dynamics, based on a size-structured population approach, and details its numerical implementation within a coupled optical–biogeochemical plankton model. Section 3 presents the model validation against available observations and the results of an extensive sensitivity analysis exploring the effects of uncertainty in asexual and sexual reproduction parameters on plankton biomass and diversity across trophic levels. Section 4 discusses the main implications of these results for plankton community structure, trophic interactions, and biogeochemical functioning, highlighting model limitations and directions for future work. Finally, Section 5 summarizes the main conclusions of the study.

2 Methods

2.1 Phenomenology of diatoms reproductive dynamics

The cell size reduction–restitution cycle (SRRC) is characteristic of most diatom species and is at the base of the McDonald-Pfitzer hypothesis (Macdonald, 1869). As cells become progressively smaller, the likelihood of sexual reproduction increases. This process typically occurs when cell size has decreased to approximately 50–20% of the maximal size (Drebes, 1977). Additional mechanisms have been proposed to explain the observations on diatoms physiology departing from this theoretical framework, such mechanisms are inter and intra specific competition (Hense and Beckmann, 2015), senescence of older cells (Jewson, 1992), lower fitness of younger cells (Bishop and Spaulding, 2017). In the asexual part of the reproduction cycle one of the two daughter cells is smaller than the other by two times the frustule width. It has already been noticed that size reduction and frustule thickness are related to cell size (Amato et al., 2005) and that inter and intraspecific frustule thickness varies widely (0.05-2.32 micrometres), (Miklasz and Denny, 2010). Observation of the pennate diatom Pseudo-nitzschia multistriata have estimated for this species a rate of apical length reduction between 0.02 and 0.5 μm depending on cell size (D'Alelio et al., 2009) which is mostly compatible with the range of frustule width measured by (Miklasz and Denny, 2010). In the following, we build upon the model introduced by (D'Alelio et al., 2010) describing the reproductive processes of Pseudo-nitzschia multistriata, and generalize it to represent a generic diatom population.

2.2 Theory based on structured population dynamics

We formulate the phenomenology of diatoms reproduction dynamics with a method based on the formalism of age distribution models, Murray (2002), where age structure in population distribution is substituted with the size parameter, in this case of diatoms. The model is based on one first-order partial differential equation. The formalism maps to the duality of waves and

https://doi.org/10.5194/egusphere-2026-1437
Preprint. Discussion started: 30 March 2026

particles, recurrent in physics, and can be analyzed with the method of characteristics, Arnol′d and Cooke (2004). The theory section is preparatory to the numerical application based on the functional diversity biogeochemical model.

2.2.1 Method of characteristics

Let $n(t,s)$ be the diatom biomass density at time t in the size range s to s+ds, $\mu(s)$, $\delta(s)$ and $\beta(s)$ are respectively the biomass growth rate, the mortality rate and the formation rate of auxosphores. In this formalization $\beta(s)$ contributes to the boundary condition $n(t,S_{MAX})$, where S_{MAX} is the size of the auxosphores, and in fact $n(t,s)$ is defined for $s \in [0,S_{MAX}]$. Therefore, the mass balance laws for the biomass can be expressed as:

$$dn = \frac{\partial n(t,s)}{\partial t}dt + \frac{\partial n(t,s)}{\partial s}ds = (\mu(s) - \delta(s) - \beta(s))\ n(t,s)\ dt \tag{1}$$

The term $\frac{\partial n}{\partial s}ds$ corresponds to the change in $n(t,s)$ due to diatoms getting smaller. Dividing Eq.1 by dt we get

$$\frac{\partial n}{\partial t} + \frac{ds}{dt}\frac{\partial n}{\partial s} = (\mu(s) - \delta(s) - \beta(s))\ n(t,s) \tag{2}$$

The rate $\frac{ds}{dt}$ can be derived from experimental data (i.e.; D'Alelio et al., 2010). From the analysis performed by D'Alelio et al. (2010) in a dedicated study for the Gulf of Naples, authors estimated approximately a range of 1-2 reproductive cycles per day during the winter bloom period and 0.1 cycles per day during the oligotrophic period such as for summer stratified conditions, co-variating with the time scale of net primary production.

The so called characteristic curves, Murray (2002), of Eq.2 are:

$$\frac{dn}{dt} = (\mu(s) - \delta(s) - \beta(s))\ n(t,s) \tag{3}$$

$$\frac{ds}{dt} = \rho(s) \tag{4}$$

Here the growth (μ), death (δ), rate of cell size decrease (ρ) and gametogenesis of auxosphores (β) are functions of size:

$$\mu(s) = \mu_{max}\ (c_\mu + b_\mu\ s - a_\mu\ s^2)$$

$$\delta(s) = \delta_0\ (c_\delta + b_\delta\ s - a_\delta\ s^2)$$

$$\rho(s) = -\omega\ s^{2.5}$$

$$\beta(s) = \beta_0\ \theta(SST - s)$$

Growth (μ) and mortality (δ) cast as parabolic functions of cell size cell size (D'Alelio et al., 2010), governed by the coefficients c_μ, b_μ, a_μ and $c_\delta, b_\delta, a_\delta$, respectively. These parameters are not central to the present analysis, as they will be replaced in the full ecosystem model described in the next section, where more complex diatom growth dynamics and the predation network are explicitly incorporated. The rate of cell size decrease (ρ, $\mu m\ d^{-1}$) follows a power-law dependence on size, such that smaller diatoms divide less. The parameter ω [$\mu m^{-\frac{3}{2}}\ d^{-1}$] controls the magnitude of size reduction per

https://doi.org/10.5194/egusphere-2026-1437
Preprint. Discussion started: 30 March 2026

reproductive cycle. The reference parameter values are taken from (D'Alelio et al., 2009; D'Alelio et al., 2010), where they were calibrated for a specific species. In the following section, perturbation experiments on these parameters are performed to assess the robustness of the dynamics and to generalize the results beyond the original species-specific setting. Gametogenesis (β) is activated when cell size falls below a prescribed sexualization size threshold (SST). This switch is formulated using a Heaviside function θ, while the actual transition rate is given by β_0.

2.2.2 Initial condition and boundary condition

To solve the problem, initial and boundary conditions are required, at t_0 the distribution of diatoms can be any function of size

$$n(t_0, s) = f(s) \tag{5}$$

At the boundaries of the 'size' domain, the following conditions are imposed:

$$n(t, S_{MAX}) = \int_{s_{min}}^{SST} \beta(s) n(t, s) ds \tag{6}$$

Where $b(s) = \beta_0$ represents the sexual reproduction rate for diatoms with size s that we assume constant, and sexualization size threshold (SST) is the size threshold below which the sexual reproduction starts.

2.2.3 Analytical solutions

Starting from Eq.4, by separating variables we obtain the expression of the characteristic curves, Fig.1:

$$s(t) = (1.5\ \omega\ t + C_0)^{-\frac{2}{3}} \tag{7}$$

where C_0 is related to initial conditions. In the analogy of wave-particle description these curves represent the tracks along which new generated cohorts of diatoms, composed of clones, evolves in their size reduction, while for Eq.7 we obtain the dynamic "along track" influenced by biomass growth, deaths and gametogenesis.

$$n(t, s) = n(t_0, S_{MAX})\ e^{\int_{s_0}^{s} [\mu(s') - \delta(s') - \beta(s')] ds'}$$

The full analytical solution requires the solution of complex integro-differential equations related to the recursive identification of initial conditions for each cohorts $n(t_0, S_{MAX})$. This task is beyond the scope of the present study where we privilege the numerical approach that allows, *inter alia*, to resolve all the complex interactions including abiotic regulations of growth predation dynamics and effects related to spatial inhomogeneities due to environmental effects such as turbulence. Therefore, this theoretical framework is used as an interpretation aid for the numerical results and to analyze the linear stability regimes in diatom populations, and in particular in term of cohorts time scale evolution as shown in Fig.1. In the Appendix, we further provide a linear stability analysis of the proposed population model.

https://doi.org/10.5194/egusphere-2026-1437
Preprint. Discussion started: 30 March 2026

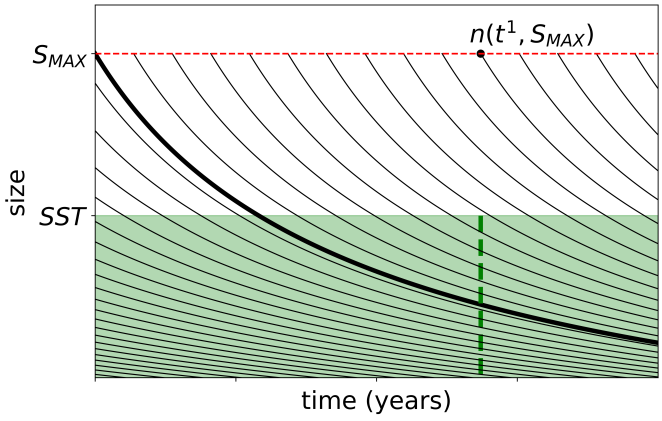

Figure 1. Characteristics for the diatoms, Eq.7. The solid line is the separatrix between the diatoms cohorts generated with gametogenesis before t_0 (below the separatrix) and the one generated after t_0 (above the separatrix). The green region highlights the size range where cells are capable of undergoing sexual reproduction. At each instant t^1 gametogenesis operates as an integral over a size range bounded by the sexualization size threshold (SST), vertical dashed green line, resulting in the generation of new auxosphores of maximal size $n(t^1, s_{max})$. In this plot the characteristics curves in black are generated with $\omega = 10^{-6}$ assuming one reproductive cycle per day, ticks on the x-axis are at annual frequency.

2.3 Numerical application in a coupled optical biogeochemical ocean framework.

To explore the ecological and biogeochemical consequences of diatom reproductive strategies at the ocean scale, we embedded the size-structured diatom life-cycle model within a spatially resolved physical–biogeochemical–ecological framework based on BFM98 model Álvarez et al. (2025). The planktonic community is represented by a set of discrete plankton functional types, structured around key traits and their trophic interactions. Among phytoplankton traits, optical properties play a central role (Dutkiewicz et al., 2015), as they determine photosynthesis and impact light propagation through the water column. By considering a multispectral framework, these properties allow niche differentiation by conferring higher fitness at particular spectral signatures (Álvarez et al., 2022; Holtrop et al., 2020; Stomp et al., 2004). Size is another key trait, used to derive physiological parameters through allometric scaling rules. Predatory interactions are also parameterized through allometric relationships, combined with experimental knowledge on prey palatability for grazers. On top of these components, the model incorporates the reproductive dynamics of diatoms, derived from the formulation introduced and presented in the previous section.

2.3.1 Optical traits

The optical traits considered in the present study include the absorption, scattering, and backscattering coefficients along the visible portion of the electromagnetic spectrum (Holtrop et al., 2020). Nine pigment-based spectra types were identified to encompass most of the optical-trait variability observed in the Mediterranean Sea (Álvarez et al., 2022), the region over which

https://doi.org/10.5194/egusphere-2026-1437
Preprint. Discussion started: 30 March 2026

the simulations presented in the Results section are performed. Two main absorption peaks stand out in the blue and red portions of the spectrum. The smallest cyanobacterial group (Prochlorococcus spp.) exhibits the highest absorption in the blue, whereas Synechococcus spp. shows relatively high absorption in intermediate wavelengths. The absorption peak in the red wavelengths is more similar across PFTs; however, its ecological relevance is reduced in marine waters due to strong absorption by water molecules in this spectral range. Scattering spectra show a less pronounced wavelength dependency and less contrast among the PFTs considered.

2.3.2 Size classes traits

Each of the phytoplankton optical types as well as the heterotrophic groups are organized into size classes. The size spectrum is discretized into bins defined on a base-2 scale (2^n) of cell biovolume (μm^3). The lower size, the width, and the nominal size of the bin are the same, which, for clarity, we converted into an equivalent spherical diameter (ESD, μm). Different taxonomic groups occupy distinct portions of this size spectrum (Fig. 2). For example, the smallest diatoms have a volume of $2^{11}\,\mu\mathrm{m}^3$ (ESD $\approx \left(\frac{6\cdot 2^{11}}{\pi}\right)^{1/3} \simeq 15.7\,\mu\mathrm{m}$), while the largest diatoms fall in the bin $2^{20}\,\mu\mathrm{m}^3$ and reach between (ESD $\simeq 126\,\mu\mathrm{m}$) and (ESD $\simeq 159\,\mu\mathrm{m}$), corresponding to a volume ratio of $2^9 \approx 512$.

Key physiological parameters are scaled to cell volume following power-law relationships identified in several studies (Tang, 1995; Irwin et al., 2006; Edwards et al., 2012). For phytoplankton, maximum growth rate follows a unimodal distribution with cell size which means that, for a given temperature, intermediate sized individuals have the largest growth rates (Marañón et al., 2013), and diatom types have larger rates than other groups of the same size (Dutkiewicz et al., 2020). Respiration rates follow a logarithmic size dependence and decrease monotonically with increasing cell size (Tang, 1995). Minimum and maximum elemental quotas (Q_{PC}^{MIN}, Q_{NC}^{MIN}, Q_{PC}^{MAX}, Q_{NC}^{MAX}) (Grover, 1989) as well as nutrient affinities for phosphorus and nitrogen (Edwards et al., 2012) are likewise derived from power-law relations. Sinking velocity is represented through a power law based on a recent review (Durante et al., 2019), which integrates data from organisms with diverse shapes to establish the link between volume and sinking rate. For microzooplankton and mesozooplankton, maximum ingestion rate scales as a power law of cell diameter (Hansen et al., 1997). A more detailed presentation of size classes and their parameters can be found in (Álvarez et al., 2025).

2.3.3 The trophic network

The prey-predator matrix has been created by including an explicit size-dependent relationship for the grazing preferences and size independent prey choices derived from experimental knowledge on prey palatability for grazers. The heterotrophic nanoflagellates (Z6) feed potentially on bacteria, pico and nano-phytoplankton, and their smaller counterparts. Microzooplankton (Z5) and the omnivorous mesozooplankton (Z4) can feed on anything and the carnivorous mesozooplankton (Z3) feed preferentially on other zooplankton. The grazing preference of a predator for each of their potential preys falls into a log-normal distribution centered on a predator:prey length ratio of 10 (Kiørboe, 2008) since optimal prey size typically corresponds to about 10% of the predator's diameter (Ward et al., 2012). As a result of the trophic network, the biomass of each diatom

https://doi.org/10.5194/egusphere-2026-1437
Preprint. Discussion started: 30 March 2026

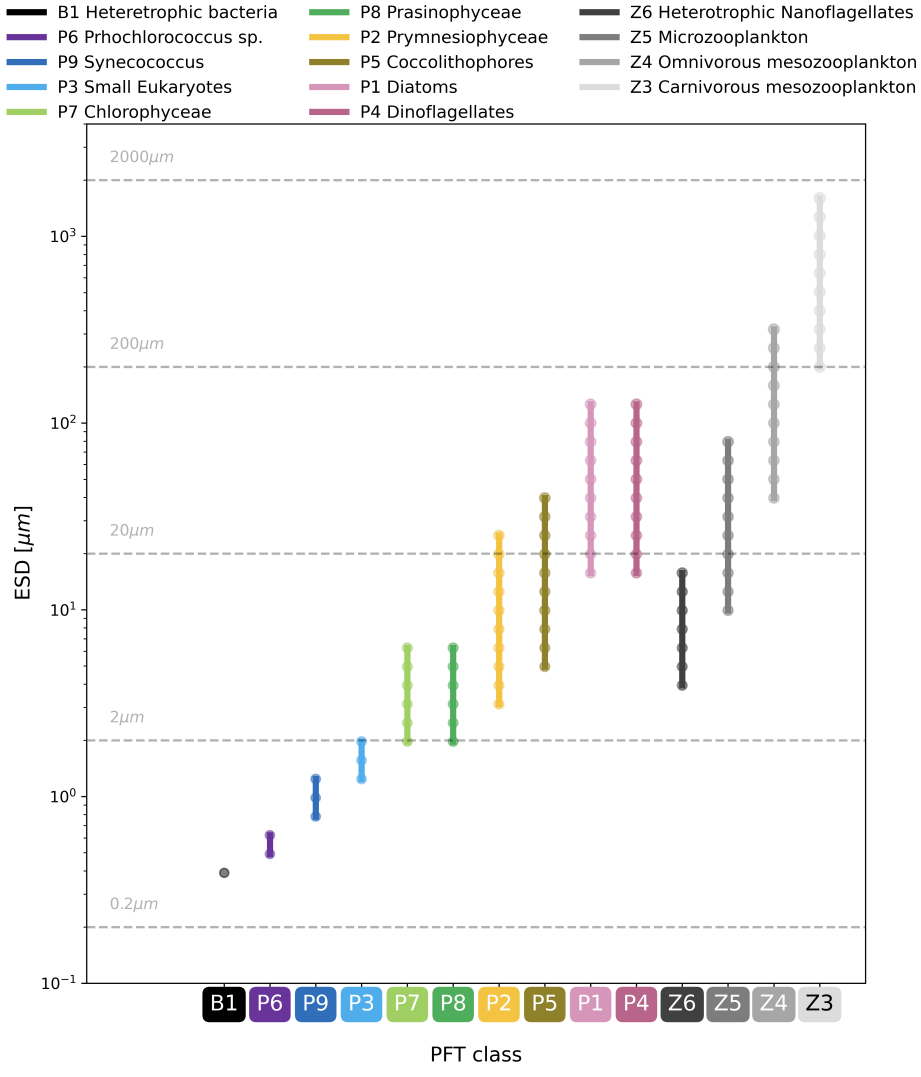

Figure 2. Equivalent Spherical Diameter (ESD, μm) ranges for plankton functional types (PFTs) used in the model. Each colored vertical segment represents the characteristic size range assigned to a given PFT class, spanning from heterotrophic bacteria (B1) and picophytoplankton (P6–P9) to phytoplankton groups (P1–P8) and progressively larger zooplankton classes (Z6–Z3). The y-axis is logarithmic; dashed horizontal lines indicate reference size scales (0.2, 2, 20, 200, and 2000 μm). For diatoms, the six smaller size classes involved in sexual reproduction are marked with pentagons.

https://doi.org/10.5194/egusphere-2026-1437
Preprint. Discussion started: 30 March 2026

size class also depends on zooplankton grazing preferences and distribution. Consequently, total diatom biomass varies with size-class distribution, which is ultimately influenced by sexual and asexual reproduction rates.

2.3.4 Diatoms reproductive strategies

To translate the formulation of diatoms reproductive strategies into the numerical model—where discretization in finite size classes is required—we grouped all the diatom cohorts, defined in continuous space $n(t,s)$, into logarithmically-spaced size clusters $n_i(t)$. $n_i(t)$ will represents the concentration of intracellular constituents associated with that size cluster or class, expressed according to the stoichiometric formulation (e.g., $mgCm^{-3}$, $mgPm^{-3}$, $mgNm^{-3}$). The effect of size reduction caused by asexual reproduction is then represented as a shrinking flux, $\Phi\big|_{S_{Ai}}$, between adjacent clusters in size space

$$n_i(t) = \int_{S_{Ai}}^{S_{Bi}} n(t,s)ds \tag{8}$$

$$\Phi\,|_{S_{Ai}} = f_{\text{NPP}} \frac{n_i(t)}{S_{Bi} - S_{Ai}} \rho(S_{Ai}) \tag{9}$$

here, S_{Ai} and S_{Bi} denote the lower and upper bounds of a given size cluster of index $i = 1, 10$, and in this implemention 10 clusters for diatoms are identified, with size range of the ESD between 15.75 μm to 126.04 μm. f_{NPP} is a factor modulating the splitting rate according to the specific net growth rate, and $\rho(S_{Ai})$ is the size-dependent size reduction rate evaluated at the lower cluster boundary. The reference value for ω, controlling the diatoms size decrease per reproductive cycle, used here is 10^{-6} $\mu m^{-1.5}$ d^{-1}. The sexual reproduction rate, which becomes active only below a size threshold corresponding to an ESD of 50 μn, is also modulated by net primary production $\beta \propto f_{\text{NPP}}$ and produces a flux from the six smallest diatom size classes toward the larger one.

3 Results

3.1 Model validation

The BFM98 model, implemented within the framework for aquatic biogeochemical models (FABM; Bruggeman and Bolding, 2014), coupled with the 1D GOTM turbulence model, has been tested at the BOUSSOLE site, in the north western Mediterranean Sea, where previous works have validated its ability to capture the main physical, biogeochemical and optical parameters (Álvarez et al., 2023), relevant indicators such as the timing of the spring bloom and the concentration of chlorophyll at the summer chlorophyll maximum (Ciavatta et al., 2025) and the representation of other components of the ecosystem such as bacteria and zooplankton (Álvarez et al., 2025). Here, we focus on the available pigment-based observations derived from the HPLC method to assess the model skill in reproducing the seasonal variability of the main phytoplankton functional groups. The comparison (Fig.3) shows that the dominant phytoplankton groups are diatoms and coccolithophores, consistently identified as such by both observations and model simulations, and characterized by a pronounced late-winter to spring maximum in March and April. Secondary groups, including dinoflagellates and prymnesiophytes, display a weaker seasonal signal and

https://doi.org/10.5194/egusphere-2026-1437
Preprint. Discussion started: 30 March 2026

a reduced contribution to total chlorophyll, with the model capturing the overall timing of their variability but underestimating their amplitude. In the observations, cyanobacteria and picoeukaryotes exhibit low biomass levels and a broader seasonal distribution, particularly during the stratified summer period; while the model reproduces their seasonal phasing, it tends to underestimate their chlorophyll concentration. Overall, the agreement between modeled and observed seasonal cycles, quantified by significant correlation coefficients for all groups, confirms the ability of the model to realistically represent the seasonal succession ($p<0.001$) of phytoplankton functional types at the BOUSSOLE site, while highlighting group-specific biases primarily affecting smaller phytoplankton classes.

3.2 Sensitivity analysis

Given the uncertainty associated with the parameters introduced in the new formulation, we performed a Monte Carlo ensemble of 1000 simulations, perturbing both asexual and sexual reproduction rates by constant multiplicative factors over a wide parameter range [0.01 to 100 for size reduction per reproductive cycle, and 0.001 to 0.1 for sexual reproduction rate], in order to assess the sensitivity of diatom biomass across size classes (Fig.4) and, in general, the impact on lower trophic levels.

For the smallest size classes (Fig.4; panels a–c), biomass exhibits low concentrations and a relatively smooth and continuous dependence on both reproduction parameters. In panels a and c, higher biomass values are generally associated with moderate increases in asexual reproduction rates. The opposite is observed in panel b. Sexual reproduction perturbations modulate biomass with decreasing effects, producing gradual gradients rather than sharp transitions. A markedly different behavior emerges for intermediate diatom's size classes (Fig.4; panels d–f), where biomass becomes strongly structured along the asexual reproduction axis. In these panels, high-biomass states are confined to a narrow band of asexual reproduction perturbations, with a non-monotonic dependence on the ω parameter, while biomass remains low elsewhere in parameter space, largely independent of sexual reproduction. This pattern indicates a threshold-like response, suggesting that intermediate-sized diatoms are particularly sensitive to changes in asexual reproduction efficiency.

For the largest size classes (Fig.4; panels g–j), the contrast becomes even more pronounced. Biomass distributions display sharp transitions and clearly separated high- and low-biomass regimes, predominantly controlled by the asexual reproduction perturbation. In these cases, sexual reproduction acts mainly as a secondary modulator, slightly shifting biomass levels within each regime but not altering the overall structure of the response. The emergence of these sharp transitions points to a highly nonlinear control of large-diatom biomass, where reproductive parameters can trigger substantial changes in population persistence and dominance. For five size classes the asexual optima occurs in a slightly leaning narrow band. As the size decrease the optima shift towards higher values which might indicates that the inflow from higher classes compensates for the higher grazing rates in smaller diatoms.

This result confirms the theoretical assumptions provided by the stability analysis. Despite the higher level of complexity, the biogeochemical model exhibits a range of instabilities shaped by sexual and asexual strategies, as previously emerged in the simpler analytical model.

The moderate influence of the sexual reproduction parameter suggests to proceed the analysis by projecting the sensitivity results onto the asexual reproduction parameter space by averaging over the full range of sexual reproduction values, Fig.5. The

https://doi.org/10.5194/egusphere-2026-1437
Preprint. Discussion started: 30 March 2026

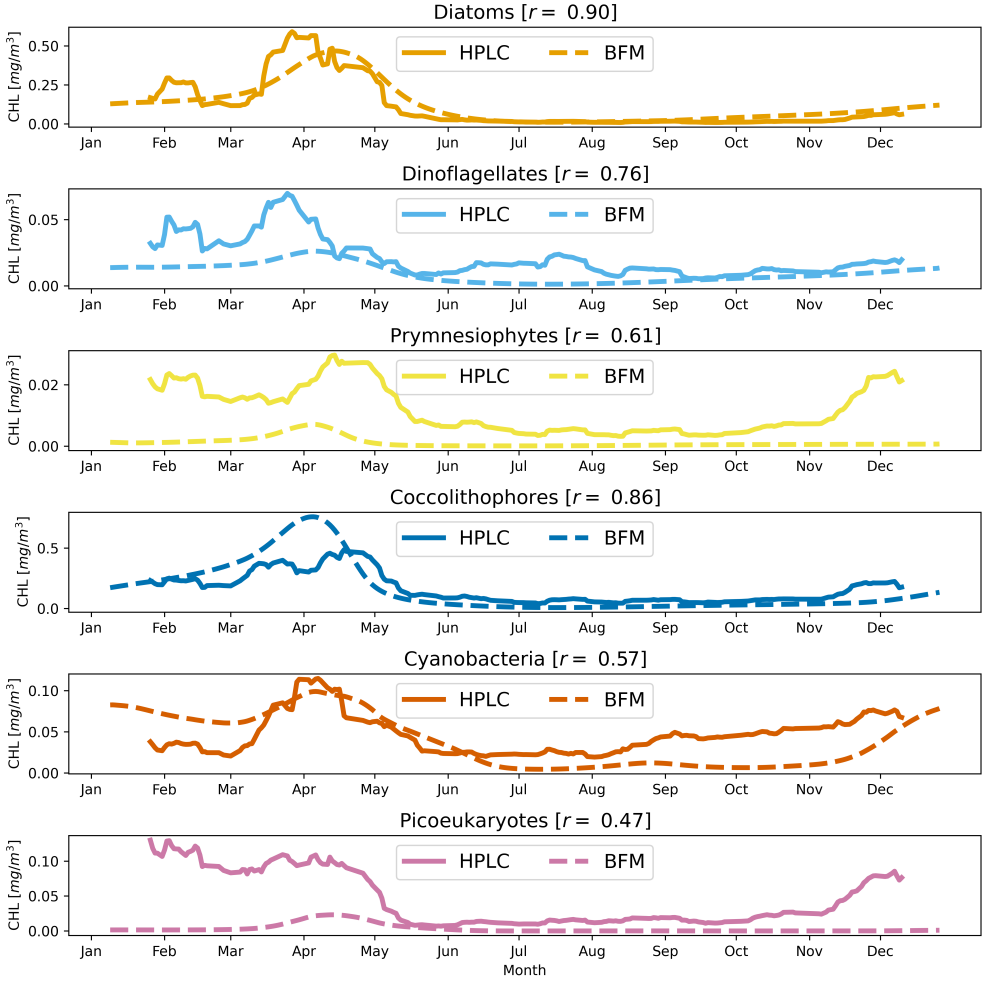

Figure 3. Validation of modelled phytoplankton functional types (PFTs) against pigment-based observations at the BOUSSOLE site. Surface seasonal cycles of chlorophyll-a concentration (CHL, mgm^{-3}) derived from HPLC pigment analysis (solid lines) are compared with corresponding model outputs (BFM, dashed lines) for diatoms, dinoflagellates, prymnesiophytes, coccolithophores, cyanobacteria, and picoeukaryotes. Time is expressed as day of year. For each PFT, Pearson correlation coefficient (r) quantify the agreement between observations and model.

resulting response of phytoplankton functional types to asexual reproduction rate perturbations is highly nonlinear and strongly group dependent, Fig.5a. Diatoms exhibit a pronounced threshold behavior: biomass remains close to its baseline value for perturbations below unity, but decreases sharply for perturbation factors larger than one, reaching a marked decrease at the upper end of the explored range. This response is accompanied by a concomitant, minor, decline in coccolithophore biomass, indicating a competitive displacement as dinoflagellates become increasingly dominant under enhanced asexual reproduction. Prymnesiophytes display a comparatively weak sensitivity, with only minor biomass changes across the parameter range.

https://doi.org/10.5194/egusphere-2026-1437
Preprint. Discussion started: 30 March 2026

Smaller phytoplankton groups, including picoeukaryotes, Synechococcus, and Prochlorococcus, show limited sensitivity to the asexual reproduction perturbation, maintaining low and nearly constant biomass levels throughout. Green algae groups also exhibit only modest variations, suggesting that their dynamics are primarily controlled by processes other than direct reproduction rate modulation in this parameter regime.

In contrast to phytoplankton, zooplankton exhibit a smoother and more monotonic response, with no sharp thresholds but clear biomass reorganizations across trophic levels, Fig.5b.

Heterotrophic nanoflagellates display only weak sensitivity to the perturbation, maintaining nearly constant biomass across the explored parameter range. This suggests that the microbial loop remains relatively stable and weakly coupled to variations in phytoplankton reproductive efficiency. Microzooplankton show a modest decline in biomass for perturbation factors larger than unity, consistent with their prey preference less impacted by shifts in diatoms.

A more pronounced response is observed for mesozooplankton. Omnivorous mesozooplankton exhibit a gradual but substantial biomass decrease as the asexual reproduction rate increases, indicating reduced trophic support or increased competition at intermediate trophic levels. Carnivorous mesozooplankton show the strongest sensitivity, with a marked biomass reduction beyond the baseline perturbation value. This behavior suggests that changes in lower trophic structure propagate upward through the food web, leading to a weakening of top predator biomass despite enhanced productivity at the phytoplankton level.

Phytoplankton diversity (Fig. 6a) exhibits a pronounced sensitivity to perturbations of the diatom size-reduction factor (SRF). For higher values of SRF a marked reorganization of the community occurs during late winter to early spring, when the Shannon index decreases in simulations characterized by larger values of size reduction rates. This transition coincides with the onset of bloom conditions and reflects a shift toward dominance by a reduced number of functional types, primarily large phytoplankton. In contrast, simulations with weaker perturbations maintain higher diversity throughout the seasonal cycle. The wide spread among ensemble members highlights the strong sensitivity of phytoplankton community structure to parameters controlling diatoms cell-size dynamics and reproductive processes. Changes in community structure are also reflected in the plankton size spectrum (Fig. 6b), expressed here as the slope of the normalized biomass size spectrum (NBSS). Observational studies have shown that marine plankton communities typically exhibit an approximately linear (in log-log axes) biomass–size relationship with a slope close to -1, reflecting an approximately even distribution of biomass across logarithmic size classes (Sheldon et al., 1972; Rodriguez and Mullin, 1986). This emergent pattern has often been interpreted as the consequence of size-dependent metabolic and ecological processes operating across trophic levels.

In the simulations, the NBSS slope exhibits a clear seasonal cycle associated with the spring bloom in April and May. During this period the slope grows and becomes temporarily flatter, indicating an increased contribution of larger organisms to total biomass. The magnitude of this shift depends on the size reduction factor: higher SRF values lead to stronger seasonal excursions of the NBSS slope. In particular, the simulation with SRF = 50 shows both the steepest, before and during the initial phases of the bloom, and the flattest values over the annual cycle, after the bloom period, suggesting that enhanced diatom division rates amplify the seasonal redistribution of biomass across size classes.

https://doi.org/10.5194/egusphere-2026-1437
Preprint. Discussion started: 30 March 2026

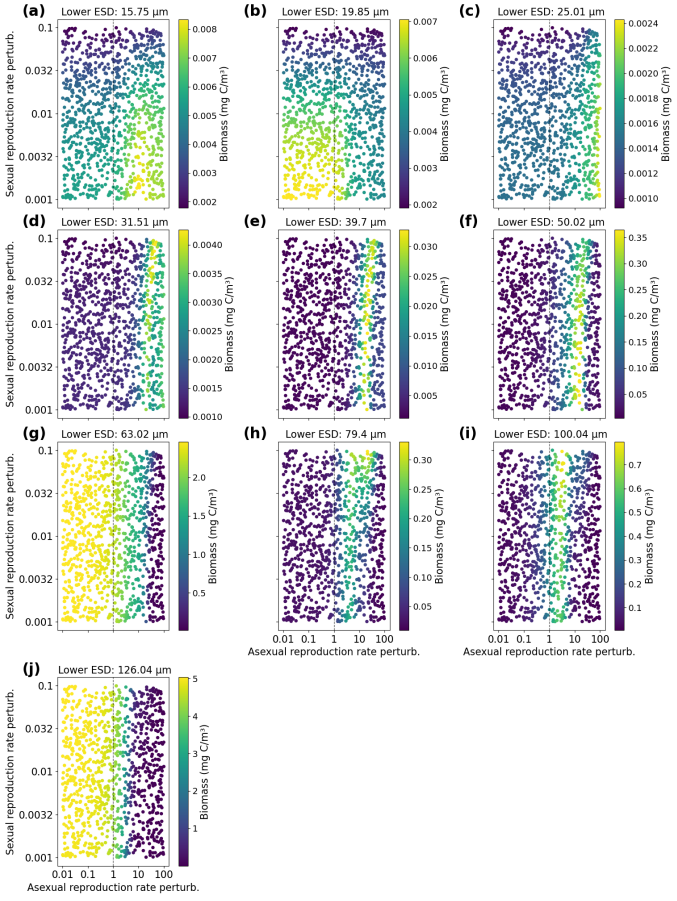

Figure 4. Sensitivity of diatom biomass to perturbations in asexual and sexual reproduction rates across different size classes. Each panel (a–j) corresponds to a diatom size class, identified by the lower bound of the Equivalent Spherical Diameter (Lower ESD, μm). Scatter points show the space–time averaged diatom biomass (color-coded, $mg\ C\ m^{-3}$) over the upper 0–200 m of the water column during the final year of a 20-year simulation, for different combinations of asexual (x-axis) and sexual (y-axis) reproduction rate perturbations. Axes are shown on logarithmic scales. Vertical reference lines indicate the unperturbed (baseline) reproduction rate. The figure highlights a strong size-dependent response of diatom biomass to reproductive parameter perturbations, with larger size classes exhibiting sharper transitions and higher biomass accumulation.

4 Discussions

The primary result of the present study is that asexual reproduction exerts a strong influence on biogeochemical dynamics, as evidenced by the present simulations, with clear signatures across all trophic levels considered. Our systematic exploration of a wide parameter space for asexual and sexual reproduction dynamics confers robustness to the results, indicating that the key biogeochemical responses persist despite uncertainty in the underlying parameterizations. In particular, results indicate that the dynamics of asexual reproduction primarily affect the balance among large phytoplankton functional types, with diatoms

https://doi.org/10.5194/egusphere-2026-1437
Preprint. Discussion started: 30 March 2026

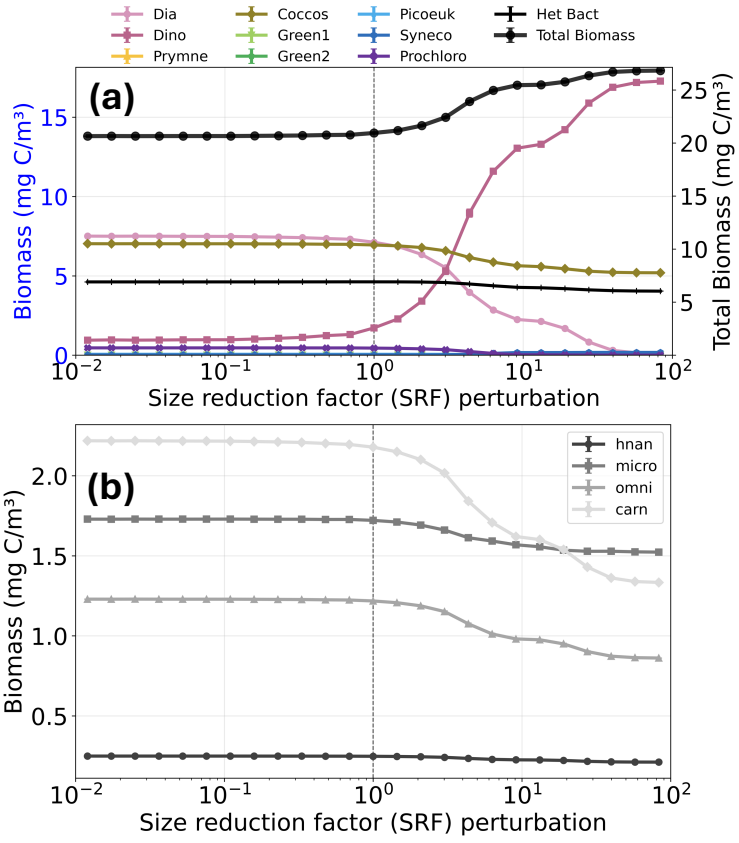

Figure 5. Biomass response to perturbations in the asexual reproduction rate, averaged over sexual reproduction variability. Each point represents the projection of model results over all values of the sexual reproduction rate, aggregated into 25 logarithmically spaced bins of the asexual reproduction rate perturbation between 0.01 and 100. Biomass is expressed in $mg\ C\ m^{-3}$, and the dashed vertical line marks the unperturbed (baseline) asexual reproduction rate. Panel (a): phytoplankton functional types, including diatoms (Dia), dinoflagellates (Dino), prymnesiophytes (Prymne), coccolithophores (Coccos), green algae (Green1, Green2), picoeukaryotes (Picoeuk), Synechococcus (Syneco), Prochlorococcus (Prochloro), heterotrophic bacteria (Het. Bact.), and total biomass expressed as the sum of bacteria and phytoplankton. All biomasses refer to the blue twin y-axis, with the exception of total biomass, which refers to the black twin y-axis. Panel (b): zooplankton functional groups, shown as the summed biomass of heterotrophic nanoflagellates (hnan), microzooplankton (micro), omnivorous mesozooplankton (omni), and carnivorous mesozooplankton (carn).

and dinoflagellates acting, clearly, as the most sensitive group. Simulations performed with the reference parameters for asexual and sexual reproduction (perturbation factor equal to 1 in Fig.4,5) lie within a regime where model results are consistent with the validation data for the examined site, with diatoms and coccolithophores emerging as the dominant organisms, Fig.3, coherently with previous results (Álvarez et al., 2023, 2025). The reference size reduction per reproductive cycle assumes ap-

https://doi.org/10.5194/egusphere-2026-1437
Preprint. Discussion started: 30 March 2026

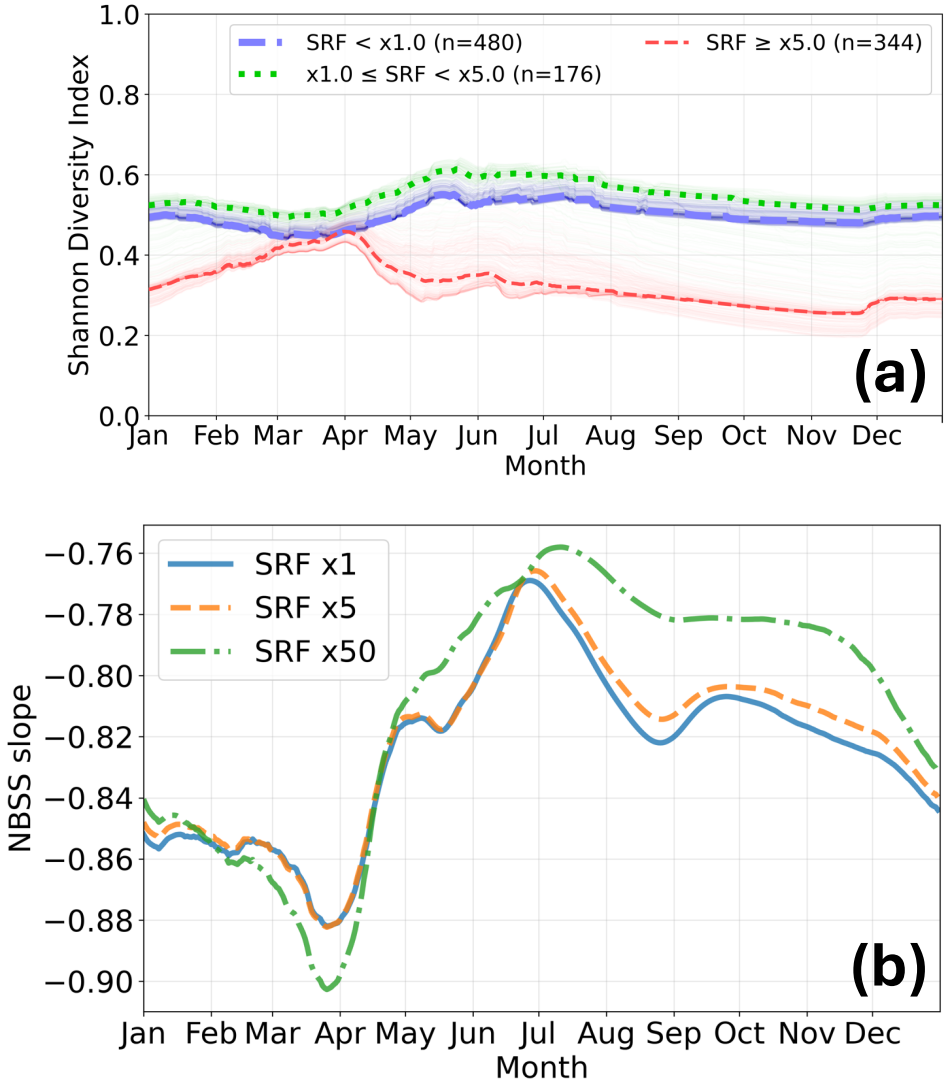

Figure 6. Seasonal variability of phytoplankton diversity and plankton size structure under different perturbations of the diatom size reduction factor (SRF). All quantities are averaged over the upper 50 m of the water column. (a) Monthly evolution of the Shannon diversity index for simulations grouped according to the value of the perturbation (SRF) to size reduction rate: low perturbation (SRF < x1), intermediate (x1 ≤ SRF < x5), and strong perturbation (SRF ≥ x5). Thin lines represent individual simulations, while thick lines show the corresponding ensemble medians. (b) Monthly evolution of the Normalized Biomass Size Spectrum (NBSS) slope for selected values of the size reduction factor perturbation (SRF = x1, x5, and x50).

https://doi.org/10.5194/egusphere-2026-1437
Preprint. Discussion started: 30 March 2026

proximately one year time scale for the cohorts to transition from maximal size to threshold reproductive scale, Fig.1. But clear transition emerges near (in logarithmic scale) the baseline parameter value, this highlights the potential for parameter changes, above the threshold, to induce substantial reorganizations of the phytoplankton community, emphasizing the importance of accurately constraining reproduction-related processes in size-structured ecosystem models. In particular, the splitting flux (Eq. 9) perturbed over the range x1–x10 explores the same order of magnitude as the diatoms net primary production of a single cohort and therefore represents the most interesting regime to explore. Increasing the splitting flux beyond this range confers a systematic advantage to competing groups, which in this model are primarily dinoflagellates. Interestingly, a transition region between diatom- and dinoflagellate-dominated states has already been observed, for example in the documented shifts during the spring bloom in the Baltic Sea, or on seasonal time scale in the Mediterranean Sea (Vascotto et al., 2024) with potentially strong impacts on ecosystem structure and functioning, Spilling et al. (2018).

Clearly, the zooplankton response reflects a bottom-up propagation of phytoplankton reorganization rather than a direct sensitivity to the reproduction parameter itself. While phytoplankton exhibit nonlinear, threshold-like behavior, zooplankton dynamics are characterized by smoother, integrated responses that translate phytoplankton dominance shifts into changes in trophic transfer efficiency and biomass partitioning across higher trophic levels. Zooplankton community structure integrates phytoplankton variability over time and trophic pathways, damping high-frequency or high-amplitude fluctuations. The limited dispersion among ensemble members further indicates that zooplankton diversity is less directly sensitive to the perturbed parameters and more constrained by trophic interactions and energy transfer efficiency.

Parameter uncertainty primarily affects community structure at the base of the food web, where competitive interactions and growth dynamics amplify relatively small parameter changes into large diversity shifts. These effects propagate upward but are progressively attenuated, leading to increased robustness of diversity metrics at higher trophic levels and for the ecosystem as a whole. This emergent stabilization underscores the importance of trophic interactions in regulating ecosystem diversity and mitigating the impacts of uncertainty in lower-level biological processes. Evaluating how reproduction parameters may be affected by climate change stressors, such as increasing temperature and changes in pH, will be important for assessing the robustness of the modeled dynamics. Several improvements to this work can be identified.

Diatom dynamics are intertwined with the allometric rules governing plankton traits and predator-prey pairing. But the grazing dynamics in the model rely on simplified representations of the trophic network, which affects the simulated phytoplankton community structure, diversity and dynamics (Prowe et al., 2012).

A caveat in the interpretation of the Shannon index is that, in the present size-structured formulation, diatom size classes are not independent taxa but dynamically connected cohorts of the same lineage. Accordingly, the index does not represent taxonomic diversity in a strict sense, but rather the distribution of biomass across functionally distinct size classes and plankton compartments. In this framework, changes in Shannon reflect community reorganization in trait space, including within-population size diversification, rather than species replacement alone. A more detailed investigation of top-down control on diatoms—particularly prey-selection switching mechanisms across different size classes (Gentleman et al., 2003; Flynn and Mitra, 2025)—should be explored in future work to further complement and refine the present study. Sexual reproduction is a widespread process Bilcke et al. (2025) and has been identified as an important mechanism linked to frustule develop-

https://doi.org/10.5194/egusphere-2026-1437
Preprint. Discussion started: 30 March 2026

ment, conferring diatoms an advantage in terms of enhanced speciation potential (Behrenfeld et al., 2012). The present model, however, is restricted to evaluating only those effects that directly influence biogeochemical fluxes within a non-evolutionary framework, while the potential evolutionary links between sexual reproduction and biogeochemical functioning remain unresolved. In particular, the size-dependent maximum division rates characteristic of bloom-forming diatoms (Behrenfeld et al., 2012). Here we neglect the asymmetry in daughter-cell production implied by the MacDonald–Pfitzer rule, as its inclusion would require a substantially more complex theoretical treatment, namely the introduction of second-order partial differential equations associated with diffusive processes in size space. We therefore focus on the average size splitting, represented by a power-law formulation that defines characteristic size trajectories for clones. Additional mechanisms could be incorporated. First, the rate of sexual reproduction may depend on the probability of cell encounters, which is not necessarily constant and can be enhanced by physical processes such as turbulence. Second, heterothallism is neglected: sexual reproduction occurs only between compatible mating types, implying that interactions are restricted to distinct groups of cells. Accounting for this constraint would likely reduce the effective rate of sexual reproduction, particularly between different phytoplankton functional types (PFTs). These issues are mitigated by the extensive sensitivity analysis perturbing rate of cell size decrease within asexual reproduction process.

Increasing the realism with which plankton physiological traits, life cycles, and trophic interactions are represented is therefore essential for improving both the predictive capacity and ecological reliability of marine ecosystem models (Flynn et al., 2025).

5 Conclusions

This study integrates a size-structured description of diatom reproductive dynamics into a coupled optical–biogeochemical plankton model to investigate their role in shaping plankton community structure, biodiversity, and biogeochemical fluxes. By explicitly representing the diatom size reduction–restitution cycle, the model establishes a mechanistic link between life-cycle processes and ecosystem-level responses.

The results show that asexual reproduction is the primary driver controlling diatom biomass moreover size structure perturbations to this parameter induce nonlinear and threshold-like responses that strongly affect phytoplankton functional composition. These changes induce a switch in dominant phytoplankton groups and propagate upward through the food web impacting diversity indexes and the trophic structure of the ecosystem.

Code and data availability. BOUSSOLE data used for validation in the present study can be accessed directly from the project webpage: https://www.obs-vlfr.fr/Boussole/ (accessed 13/03/2026). The code is maintained in the public GitHub repository of FABM-plus (https://github.com/fabm-model/fabm-plus).

https://doi.org/10.5194/egusphere-2026-1437
Preprint. Discussion started: 30 March 2026

Appendix A: Linear stability analysis

If we want to study the response of the system to perturbation we can write (1) in the form:

$$\frac{\partial n}{\partial t} = \omega s^{\alpha} \frac{\partial n}{\partial s} + M(s)\, n(t,s) \tag{A1}$$

Where we have used (3) and called for simplicity M(s) as $\mu(s) - \delta(s) - \beta(s)$. Now, considering the solution as a combination of the averaged value and a perturbation

$$n(t,s) = \bar{n} + \delta n(t,s)$$

Equation (13) then becomes

$$\frac{\partial \bar{n}}{\partial t} + \frac{\partial \delta n}{\partial t} = \omega s^{\alpha} \frac{\partial \delta n}{\partial s} + \omega s^{\alpha} \frac{\partial \bar{n}}{\partial s} + M(s)\, \bar{n} + M(s)\, \delta n$$

Considering that $\bar{n}$ doesn't depend on t and that still has to be valid the equation

$$0 = \omega s^{\alpha} \frac{\partial \bar{n}}{\partial s} + M(s)\, \bar{n} \tag{A2}$$

We obtain for the perturbation δn

$$\frac{\partial \delta n}{\partial t} = \omega s^{\alpha} \frac{\partial \delta n}{\partial s} + M(s)\, \delta n \tag{A3}$$

Considering the solution with the form

$$\delta n(t,s) = C_{\sigma}(t) e^{iqs}$$

Then now we obtain an ODE with respect to the amplitude of the perturbation

$$\frac{dC_{\sigma}}{dt}\, e^{iqs} = i\omega q s^{\alpha} C_{\sigma}(t)\, e^{iqs} + M(s)\, C_{\sigma}(t)\, e^{iqs} \tag{A4}$$

Dividing by e^{iqs} we obtain:

$$\frac{dC_{\sigma}}{dt} = (i\omega q s^{\alpha} + M(s))\, C_{\sigma}(t) \tag{A5}$$

That leads to a solution for $C_{\sigma}(t)$ in the form:

$$C_{\sigma}(t) = A e^{\sigma t} = A e^{i\omega q s^{\alpha} t} e^{M(s)t} \tag{A6}$$

Then, while the first exponential represent an oscillation, the second one detects the condition for stability:

$$M(s) < 0 \tag{A7}$$

Being M(s) a second-order polynomial, we found that the stability depends by the parameters in $\mu(s)$, $\delta(s)$, and $\beta(s)$ equations, which shapes the growth rate, the death rate, and gametogenesis. In particular, we found that for a range of sizes defined by these parameters, the system exhibits linear instabilities. These results suggest that linear instabilities can emerge in the system for a given range of sizes, shaped by the parameters.

https://doi.org/10.5194/egusphere-2026-1437
Preprint. Discussion started: 30 March 2026

Author contributions. P.L. and I.V. conceived the study and developed the conceptual framework. P.L., E.Á. and G.O. developed the model and implemented the software. P.L. performed the simulations and conducted the formal analysis. F.D. performed the mathematical analysis. P.L. wrote the original draft of the manuscript. All authors discussed the results and contributed to the final version of the manuscript.

Competing interests. No competing interests are present.

Acknowledgements. This research was supported by the National Biodiversity Future Center NFBC project: National Recovery and Resilience Plan (NRRP), Mission 4 Com- ponent 2 Investment 1.4 – Call for tender No. 3138 of 16 Decem- ber 2021, rectified by Decree no. 3175 of 18 December 2021 of Ital- ian Ministry of University and Research funded by the European Union – NextGenerationEU. This research has been supported by the EU Horizon Europe Digital, Industry and Space project NECCTON (grant no. 101081273).

https://doi.org/10.5194/egusphere-2026-1437
Preprint. Discussion started: 30 March 2026

References

Amato, A., Orsini, L., D'Alelio, D., and Montresor, M.: Life cycle, size reduction patterns, and ultrastructure of the pennate planktonic diatom Pseudo-nitzschia delicatissima (Bacillariophyceae) 1, Journal of Phycology, 41, 542–556, https://doi.org/10.1111/j.1529-8817.2005.00080.x, 2005.

Arnol′d, V. I. and Cooke, R.: Lectures on partial differential equations, Universitext, Springer Phasis, Berlin Moscow, ISBN 9783540404484, 2004.

Behrenfeld, M. J., Halsey, K. H., Boss, E., Karp-Boss, L., Milligan, A. J., and Peers, G.: Thoughts on the evolution and ecological niche of diatoms, 91, e01 457, https://doi.org/10.1002/ecm.1457, 2012.

Bilcke, G., Campese, L., Annunziata, R., Amadei Martínez, L., Borgonuovo, C., Rijsdijk, N., Chaerle, P., Van Den Berge, K., D'hondt, S., Iudicone, D., Montresor, M., Ferrante, M. I., Vandepoele, K., and Vyverman, W.: Conserved genetic markers reveal widespread diatom sexual reproduction in the global ocean, 16, 10 029, https://doi.org/10.1038/s41467-025-65296-9, 2025.

Bishop, I. W. and Spaulding, S. A.: Life cycle size dynamics in Didymosphenia geminata (Bacillariophyceae), Journal of phycology, 53, 652–663, https://doi.org/10.1111/jpy.12528, 2017.

Bruggeman, J. and Bolding, K.: A general framework for aquatic biogeochemical models, Environmental Modelling & Software, 61, 249–265, https://doi.org/10.1016/j.envsoft.2014.04.002, 2014.

Chepurnov, V. A., Mann, D. G., Sabbe, K., and Vyverman, W.: Experimental Studies on Sexual Reproduction in Diatoms, in: International Review of Cytology, vol. 237, pp. 91–154, Elsevier, ISBN 9780123646415, https://doi.org/10.1016/S0074-7696(04)37003-8, 2004.

Ciavatta, S., Lazzari, P., Álvarez, E., Bertino, L., Bolding, K., Bruggeman, J., Capet, A., Cossarini, G., Daryabor, F., Nerger, L., Popov, M., Skákala, J., Spada, S., Teruzzi, A., Wakamatsu, T., Yumruktepe, V., and Brasseur, P.: Control of simulated ocean ecosystem indicators by biogeochemical observations, Progress in Oceanography, 231, 103 384, https://doi.org/10.1016/j.pocean.2024.103384, 2025.

Clerc, C., Bopp, L., Benedetti, F., Knecht, N., Vogt, M., and Aumont, O.: Effects of Mesozooplankton Growth and Reproduction on Plankton and Organic Carbon Dynamics in a Marine Biogeochemical Model, Global Biogeochemical Cycles, 38, e2024GB008 153, https://doi.org/10.1029/2024GB008153, 2024.

D'Alelio, D., d'Alcalà, M. R., Dubroca, L., , D. S., Zingone, A., and Montresor, M.: The time for sex: A biennial life cycle in a marine planktonic diatom, Limnology and Oceanography, 55, 106–114, https://doi.org/10.4319/lo.2010.55.1.0106, 2010.

Drebes, G.: Sexuality, vol. 13, University of California Press, botanical monographs edn., ISBN 5885141460, 1977.

Durante, G., Basset, A., Stanca, E., and Roselli, L.: Allometric scaling and morphological variation in sinking rate of phytoplankton, 55, 1386–1393, https://doi.org/10.1111/jpy.12916, 2019.

Dutkiewicz, S., Hickman, A. E., Jahn, O., Gregg, W. W., Mouw, C. B., and Follows, M. J.: Capturing optically important constituents and properties in a marine biogeochemical and ecosystem model, Biogeosciences, 12, 4447–4481, https://doi.org/10.5194/bg-12-4447-2015, 2015.

Dutkiewicz, S., Cermeno, P., Jahn, O., Follows, M. J., Hickman, A. E., Taniguchi, D. A. A., and Ward, B. A.: Dimensions of marine phytoplankton diversity, 17, 609–634, https://doi.org/10.5194/bg-17-609-2020, 2020.

D'Alelio, D., Amato, A., Luedeking, A., and Montresor, M.: Sexual and vegetative phases in the planktonic diatom Pseudo-nitzschia multistriata, Harmful Algae, 8, 225–232, https://doi.org/10.1016/j.hal.2008.05.004, 2009.

Edwards, K. F., Thomas, M. K., Klausmeier, C. A., and Litchman, E.: Allometric scaling and taxonomic variation in nutrient utilization traits and maximum growth rate of phytoplankton, 57, 554–566, https://doi.org/10.4319/lo.2012.57.2.0554, 2012.

https://doi.org/10.5194/egusphere-2026-1437
Preprint. Discussion started: 30 March 2026

Flynn, K. J. and Mitra, A.: Why Plankton Modelers Should Reconsider Using Rectangular Hyperbolic (Michaelis-Menten, Monod) Descriptions of Predator-Prey Interactions, 3, https://doi.org/10.3389/fmars.2016.00165, 2025.

Flynn, K. J., Atkinson, A., Beardall, J., Berges, J. A., Boersma, M., Brunet, C., Calbet, A., Caron, D. A., Dam, H. G., Glibert, P. M., Hansen, P. J., Jin, P., Lønborg, C., Mayor, D. J., Menden-Deuer, S., Mock, T., Mulholland, M. R., Needham, D. M., Polimene, L., Poulton, A. J., Robinson, C., Rokitta, S. D., Rost, B., Saiz, E., Scanlan, D. J., Schmidt, K., Sherr, E., Stoecker, D. K., Svensen, C., Thiele, S., Thingstad, T. F., and Våge, S.: More realistic plankton simulation models will improve projections of ocean ecosystem responses to global change, Nature Ecology & Evolution, 9, 1562–1570, https://doi.org/10.1038/s41559-025-02788-3, 2025.

Gentleman, W., Leising, A., Frost, B., Strom, S., and Murray, J.: Functional responses for zooplankton feeding on multiple resources: a review of assumptions and biological dynamics, Deep Sea Research Part II: Topical Studies in Oceanography, 50, 2847–2875, https://doi.org/10.1016/j.dsr2.2003.07.001, 2003.

Grover, J. P.: INFLUENCE OF CELL SHAPE AND SIZE ON ALGAL COMPETITIVE ABILITY [1], 25, 402–405, https://doi.org/10.1111/j.1529-8817.1989.tb00138.x, 1989.

Hansen, P. J., Bjørnsen, P. K., and Hansen, B. W.: Zooplankton grazing and growth: Scaling within the 2-2,-μm body size range, 42, 687–704, https://doi.org/10.4319/lo.1997.42.4.0687, 1997.

Hense, I. and Beckmann, A.: A theoretical investigation of the diatom cell size reduction–restitution cycle, Ecological Modelling, 317, 66–82, https://doi.org/10.1016/j.ecolmodel.2015.09.003, 2015.

Holtrop, T., Huisman, J., Stomp, M., Biersteker, L., Aerts, J., Grébert, T., Partensky, F., Garczarek, L., and Woerd, H. J. V. D.: Vibrational modes of water predict spectral niches for photosynthesis in lakes and oceans, Nature Ecology & Evolution, 5, 55–66, https://doi.org/10.1038/s41559-020-01330-x, 2020.

Irwin, A. J., Finkel, Z. V., Schofield, O. M. E., and Falkowski, P. G.: Scaling-up from nutrient physiology to the size-structure of phytoplankton communities, 28, 459–471, https://doi.org/10.1093/plankt/fbi148, 2006.

Jewson, D. H.: Size reduction, reproductive strategy and the life cycle of a centric diatom, Philosophical Transactions of the Royal Society of London. Series B: Biological Sciences, 336, 191–213, https://doi.org/10.1098/rstb.1992.0056, 1992.

Johanson, A. N., Oschlies, A., Hasselbring, W., and Worm, B.: SPRAT: A spatially-explicit marine ecosystem model based on population balance equations, Ecological Modelling, 349, 11–25, https://doi.org/10.1016/j.ecolmodel.2017.01.020, 2017.

Kiørboe, T.: A mechanistic approach to plankton ecology, Princeton University Press, Princeton, ISBN 9780691134222, 2008.

Litchman, E., Klausmeier, C. A., and Yoshiyama, K.: Contrasting size evolution in marine and freshwater diatoms, Proceedings of the National Academy of Sciences, 106, 2665–2670, https://doi.org/10.1073/pnas.0810891106, 2009.

Macdonald, J. D.: I.—On the structure of the Diatomaceous frustule, and its genetic cycle, Journal of Natural History, 3, 1–8, https://doi.org/10.1080/00222936908695866., 1869.

Marañón, E., Cermeño, P., López-Sandoval, D. C., Rodríguez-Ramos, T., Sobrino, C., Huete-Ortega, M., Blanco, J. M., and Rodríguez, J.: Unimodal size scaling of phytoplankton growth and the size dependence of nutrient uptake and use, Ecology Letters, 16, 371–379, https://doi.org/10.1111/ele.12052, 2013.

Miklasz, K. A. and Denny, M. W.: Diatom sinkings speeds: Improved predictions and insight from a modified Stokes' law, Limnology and Oceanography, 55, 2513–2525, https://doi.org/doi.org/10.4319/lo.2010.55.6.2513, 2010.

Murray, J. D., ed.: Mathematical Biology: I. An Introduction, vol. 17 of *Interdisciplinary Applied Mathematics*, Springer New York, New York, NY, ISBN 9780387952239 9780387224374, https://doi.org/10.1007/b98868, 2002.

https://doi.org/10.5194/egusphere-2026-1437
Preprint. Discussion started: 30 March 2026

Prowe, A. F., Pahlow, M., Dutkiewicz, S., Follows, M., and Oschlies, A.: Top-down control of marine phytoplankton diversity in a global ecosystem model, Progress in Oceanography, 101, 1–13, https://doi.org/10.1016/j.pocean.2011.11.016, 2012.

Reynolds, C. S.: The ecology of phytoplankton, Cambridge University Press, ISBN 1139454897, https://doi.org/10.1017/CBO9780511542145, 2006.

Rodriguez, J. and Mullin, M. M.: Relation between biomass and body weight of plankton in a steady state oceanic ecosystem1, Limnology and Oceanography, 31, 361–370, https://doi.org/10.4319/lo.1986.31.2.0361, 1986.

Roshchin, A. M. and Khauilov, K.: Zhiznennye tsikly diatomovykh vodorosleui, Naukova dumka, 1994.

Sheldon, R. W., Prakash, A., and Sutcliffe, W. H.: THE SIZE DISTRIBUTION OF PARTICLES IN THE OCEAN1, Limnology and Oceanography, 17, 327–340, https://doi.org/10.4319/lo.1972.17.3.0327, 1972.

Sieburth, J. M., Smetacek, V., and Lenz, J.: Pelagic ecosystem structure: Heterotrophic compartments of the plankton and their relationship to plankton size fractions 1, Limnology and oceanography, 23, 1256–1263, https://doi.org/10.4319/lo.1978.23.6.1256, 1978.

Spilling, K., Olli, K., Lehtoranta, J., Kremp, A., Tedesco, L., Tamelander, T., Klais, R., Peltonen, H., and Tamminen, T.: Shifting Diatom—Dinoflagellate Dominance During Spring Bloom in the Baltic Sea and its Potential Effects on Biogeochemical Cycling, 5, 327, https://doi.org/10.3389/fmars.2018.00327, 2018.

Stomp, M., Huisman, J., De Jongh, F., Veraart, A. J., Gerla, D., Rijkeboer, M., Ibelings, B. W., Wollenzien, U. I. A., and Stal, L. J.: Adaptive divergence in pigment composition promotes phytoplankton biodiversity, Nature, 432, 104–107, https://doi.org/10.1038/nature03044, 2004.

Stosch, H.: Manipulierung der Zellgröße von Diatomeen im experiment, Phycologia, 5, 21–44, 1965.

Tang, E. P.: The allometry of algal growth rates, Journal of Plankton Research, 17, 1325–1335, https://doi.org/10.1093/plankt/17.6.1325, 1995.

Vascotto, I., Bernardi Aubry, F., Bastianini, M., Mozetič, P., Finotto, S., and Francé, J.: Exploring the mesoscale connectivity of phytoplankton periodic assemblages' succession in northern Adriatic pelagic habitats, Science of The Total Environment, 913, 169 814, https://doi.org/10.1016/j.scitotenv.2023.169814, 2024.

Ward, B. A., Dutkiewicz, S., Jahn, O., and Follows, M. J.: A size-structured food-web model for the global ocean, 57, 1877–1891, https://doi.org/10.4319/lo.2012.57.6.1877, 2012.

Álvarez, E., Lazzari, P., and Cossarini, G.: Phytoplankton diversity emerging from chromatic adaptation and competition for light, Progress in Oceanography, 204, 102 789, https://doi.org/10.1016/j.pocean.2022.102789, 2022.

Álvarez, E., Cossarini, G., Teruzzi, A., Bruggeman, J., Bolding, K., Ciavatta, S., Vellucci, V., D'Ortenzio, F., Antoine, D., and Lazzari, P.: Chromophoric dissolved organic matter dynamics revealed through the optimization of an optical–biogeochemical model in the northwestern Mediterranean Sea, Biogeosciences, 20, 4591–4624, https://doi.org/10.5194/bg-20-4591-2023, 2023.

Álvarez, E., Occhipinti, G., Cossarini, G., Solidoro, C., and Lazzari, P.: Modeling plankton diversity in a coupled optical-biogeochemical ocean framework, 13, 1504 518, https://doi.org/10.3389/fevo.2025.1504518, 2025.